16

Model for Predicting Topographic Changes on Coast Composed of Sand of Mixed Grain Size and Its Applications

Takaaki Uda[1] and Masumi Serizawa[2]
[1]*Dr. Eng., Executive Director, Public Works Research Center, 1-6-4 Taito, Taito-ku, Tokyo 110-0016,*
[2]*Coastal Engineering Laboratory Co., Ltd., 301, 1-22 Wakaba, Shinjuku, Tokyo 160-0011 Japan*

1. Introduction

In beach nourishment, predicting the changes in the longitudinal profile is important for estimating the effect of nourishment. When material composed of not only coarse sand but also fine sand is used in beach nourishment, a considerable amount of fine sand may be lost owing to offshore sand transport by waves, depending on the conditions of the beach slope. On the basis of the contour-line-change model proposed by Serizawa et al. (2003), which was derived using the concept of the equilibrium slope (Bakker, 1968), Uda et al. (2004) developed a model for predicting the change in the longitudinal profile as well as the change in the grain size distribution. Then, the model was applied to the results of the movable bed experiment using a large wave tank, in which the model beach was composed of sand of mixed grain size, to evaluate the model applicability (Fukuhama et al., 2007). The experimental results showed that sand of mixed grain size was sorted into fine and coarse sand, and that coarse sand was transported shoreward, forming a berm, whereas fine sand sunk to a zone deeper than the depth of closure. Although the experimental and predicted results were in good agreement in this application, the applicability of the model to the coasts was still inadequate. Therefore, the model was applied to the following two model cases: beach changes associated with the beach nourishment using fine and coarse materials on the Chigasaki coast in Kanagawa Prefecture, Japan (Yoshioka et al., 2008), and the formation of a 'conveyer belt' composed of gravel and fine sand observed on the Shimizu coast (Nishitani et al., 2008). In this paper, these applications of the model are summarized and the effectiveness of the model is shown.

2. Numerical model

A typical example of the grain size sorting is found at Pebble Beach in Cardiff, UK, where gravel accumulates and forms a gravel layer near the shoreline with the offshore bed being composed of only fine sand, as shown in Fig. 1 (Uda et al., 2004). The original concept of a model for predicting the changes in the longitudinal profile and grain size distribution was obtained from this observation.

Fig. 1. Sorting of grain size at Pebble Beach in Cardiff, UK, where gravel accumulates and forms gravel layer near shoreline

Consider a longitudinal profile and set the equilibrium slopes of gravel and fine sand as $\tan\beta_1$ and $\tan\beta_2$, respectively, as shown in Fig. 2. When sand of mixed grain size is supplied to a beach with an initial slope of $\tan\theta$, cross-shore sand movement occurs; thus, the slopes of coarse and fine sand materials tend to approach $\tan\beta_1$ and $\tan\beta_2$, respectively. In this case, the landward limit of beach changes is determined by the berm height, h_R, whereas in the offshore zone, sand is transported until the depth of closure, h_c, beyond which sand falls into a deeper zone while maintaining the repose angle of sand, $\tan\gamma$.

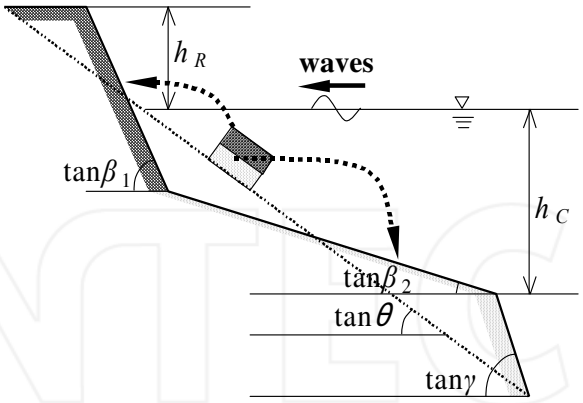

Fig. 2. Schematic diagram of concept of equilibrium slope corresponding to each grain size

Using the above concept, a numerical model was developed on the basis of the contour-line-change model proposed by Serizawa et al. (2003). Let the x- and z-axes be the longshore distance and depth, respectively, and Y, the offshore distance to a specific contour line. To consider the sorting of sand of different grain sizes by cross-shore sand transport, the depth distribution of cross-shore sand transport considering the grain size effect in mixing is required. We, therefore, expanded the cross-shore sand transport equation given by

Serizawa et al. (2003), which took into account the stabilization mechanism of the longitudinal profile, as reported by Bakker (1968).

Let β_c be the angle of the equilibrium beach slope at which the shoreward motion of the sand particle owing to wave action is balanced by the seaward motion due to gravity, and it is assumed that seaward sand transport occurs when angle β of the seabed slope exceeds β_c, and that shoreward sand transport occurs when angle β becomes smaller than β_c. The strength of cross-shore sand transport in restoring the equilibrium slope is assumed to be proportional to the wave energy dissipation rate per unit seabed length, Φ, calculated as the shoreward component of energy flux at the breaking point, F_y, divided by the seabed length $S \cong (h_C + h_R)/\sin\overline{\beta}$, between the depth of closure, h_C, and the berm height, h_R. $\overline{\beta}$ is the average initial slope angle between h_C and h_R. In addition, by approximately assuming β_c for $\overline{\beta}$, $1/(h_C + h_R)$ is replaced by the intensity distribution function of cross-shore sand transport, $\varepsilon_z(z)$, which is assumed to be equivalent to the depth distribution of the longshore sand transport rate, $\varepsilon_x(z)$, given by Uda and Kawano (1996). Thus, this transport becomes

$$q_z = \varepsilon_z(z) \cdot K_z \cdot (EC_g)_b \cos^2\alpha_{bs} \sin\beta_c \cdot \left(\frac{\cot\beta}{\cot\beta_c} - 1 \right) , \tag{1}$$

$$\cot\beta = -\frac{\partial Y}{\partial z} \quad . \tag{2}$$

The cross-shore transport of sand composed of mixed grain size can be modeled by expanding the concept of single grain size. The sorting of grain size populations, such as those of fine sand, medium and coarse sand, and gravel, can be modeled by introducing the equilibrium slope angle $\beta_c^{(k)}$ which corresponds to each grain size population k. In this case, a grain size population is assumed to have a single equilibrium beach slope with a characteristic grain size $d^{(k)}$, for example, the median diameter of the grain size population.

By assuming that the mobility of sand of each grain size population by cross-shore movement under the same wave conditions is the same as that of longshore sand transport, the coefficient of the sediment transport rate according to the grain size $d^{(k)}$, which was given by Kamphius et al. (1986) and Kumada et al. (2003), is introduced. Furthermore, assuming that the ratio of the exposed area of each grain size population to the entire sea bottom area is equal to the content of each size population in the exchange layer $\mu^{(k)}$ (where k=1, 2, …, N), the cross-shore sand transport rate of each grain size population $q_z^{(k)}$ is derived by a method similar to that of Uda et al. (2004).

Cross-shore sand transport

$$q_z^{(k)} = \mu^{(k)} \cdot \varepsilon_z(z) \cdot \gamma \cdot K_1^{(k)} \cdot (EC_g)_b \cos^2\alpha_{bs} \sin\overline{\beta} \cdot (\cot\beta / \cot\beta_c^{(k)} - 1); k = 1, 2, \ldots, N \tag{3}$$

$$K_1^{(k)} = \frac{A}{\sqrt{d^{(k)}}} \tag{4}$$

$$\cot\beta = -\partial Y / \partial z \tag{5}$$

$$\varepsilon_z(z) = \begin{cases} \left(2/h_C^3\right)\left(h_C/2 - z\right)\left(z + h_C\right)^2, & -h_C \le z \le h_R \\ 0, & z \le -h_C,\ z \ge h_R \end{cases} \tag{6}$$

Here, $q_z^{(k)}(k = 1, \cdots, N)$ is the cross-shore sand transport per unit length in the longshore direction for each grain size population, $\mu^{(k)}$ is the content of each grain size population (k) in the exchange layer of sand, $\varepsilon_z(z)$ is assumed to be equivalent to the depth distribution of the longshore sand transport $\varepsilon_x(z)$ given by Uda and Kawano (1996), and $d^{(k)}$ is a typical grain size of the grain size population. A is a coefficient that depends on the physical conditions of the beach, $d^{(k)}$ in Eq. (4) has a unit of mm, γ is the ratio of the coefficient of cross-shore sand transport to the coefficient of longshore sand transport, and expresses the mobility of cross-shore sand transport relative to that of longshore sand transport, α_{bs} is the angle between the wave crest line at the breaking point and each contour line, and β is the beach slope angle at each contour line. $\bar{\beta}$ is the average beach slope angle between the berm height h_R and the depth of closure h_c, and $\beta_C^{(k)}$ is the equilibrium beach slope angle. When the beach slope becomes steeper than the angle of repose of sand, sand is transported offshore by gravity. By this procedure, we can calculate the formation of a scarp in a zone larger than the berm height h_R and the sinking of sand in a zone larger than the depth of closure h_c.

Longshore sand transport

$$q_x^{(k)} = \mu^{(k)} \cdot \varepsilon_x(z) \cdot K_1^{(k)} \cdot (EC_g)_b \cdot \left(\cos\alpha_{bs} \sin\alpha_{bs} - \xi \frac{1}{\tan\beta} \cdot \cos\alpha_{bs} \cdot \frac{\partial H_b}{\partial x} \right) \tag{7}$$

Here, $q_x^{(k)}(k = 1, \cdots, N)$ is the longshore sand transport per unit depth for each grain size population, $\varepsilon_x(z)$ is the depth distribution of longshore sand transport, and ξ is the constant given by $K_2^{(k)}/K_1^{(k)}$, which depends on the physical conditions of the beach, where $K_2^{(k)}$ is a function of $K_1^{(k)}$ and is equivalent to the coefficient of Ozasa and Brampton (1980). $\tan\beta$ is the beach slope in the surf zone and H_b is the breaker height.

Mass conservation for each grain size

$$\frac{\partial y^{(k)}}{\partial t} = -\frac{\partial q_x^{(k)}}{\partial x} - \frac{\partial q_z^{(k)}}{\partial z} \quad ; k = 1, 2, \ldots, N \tag{8}$$

The total contour line change at a certain position is determined by the summation of the contour line changes of all grain size populations at that position.

$$\frac{\partial Y}{\partial t} = \sum_{k=1}^{N} \frac{\partial y^{(k)}}{\partial t} \tag{9}$$

Change in content of each grain size population

$$\frac{\partial \mu^{(k)}}{\partial t} = \frac{1}{B}\left\{ \frac{\partial y^{(k)}}{\partial t} - \frac{\partial Y}{\partial t} \cdot \mu^{(k)} \right\} \quad ; k = 1, 2, \ldots, N. \tag{10}$$

The content of each grain size population in the new exchange layer formed during erosion is expressed as

$$\frac{\partial \mu^{(k)}}{\partial t} = \frac{1}{B}\left\{\frac{\partial y^{(k)}}{\partial t} - \frac{\partial Y}{\partial t}\cdot \mu_B^{(k)}\right\}, \tag{11}$$

where $\mu_B^{(k)}$ is the content of each grain size population on the sandy beach landward of the initial exchange layer. The width B of the exchange layer is determined with reference to the mixing depth reported by Kraus (1985). The above-mentioned equations were solved simultaneously.

3. Validation using experimental results

3.1 Experiment using large wave tank and sand of mixed grain size

We first investigated the applicability of the present model to experiments using sand of mixed grain size, in which the changes in the longitudinal profile and cross-shore grain size distribution were investigated in a large wave tank. A movable bed experiment using sand of mixed grain size ranging widely from medium sand to silt was carried out using a 135-m-long, 2-m-wide and 5-m-deep wave tank to study the formative processes of an equilibrium beach and the grain size distribution (Meguro et al., 2005). The median diameter of grain size used was d_{50} =0.62 mm and the initial uniform slope was 1/20. Regular waves with a height of 0.6 m and a period of 3.5 s were generated for 78 h.

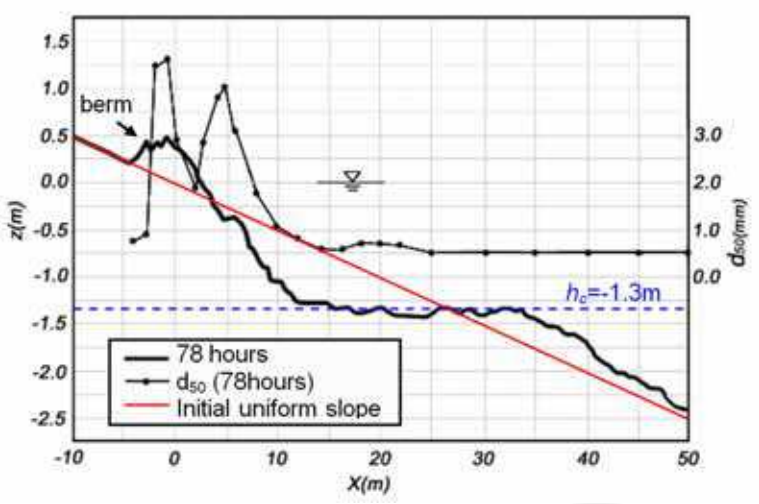

Fig. 3. Change in longitudinal profile and cross-shore distribution of d_{50} in experiment using large wave tank (Meguro et al., 2005)

Figure 3 shows the changes in the longitudinal profile and cross-shore distribution of d_{50} on the seabed. A flat seabed was formed by erosion at a depth of h_c=1.3 m on the initial uniform slope, and a steep foreshore with a slope of 1/6 was formed. The flat seabed near the depth h_c was covered with fine sand, whereas coarse sand selectively accumulated on the foreshore. From these findings, it is clear that sand of mixed grain size is sorted by wave action, with

coarse sand being deposited on the foreshore, forming a berm with a steep slope, and fine sand being transported offshore and deposited to form a gentle slope on the offshore bed.

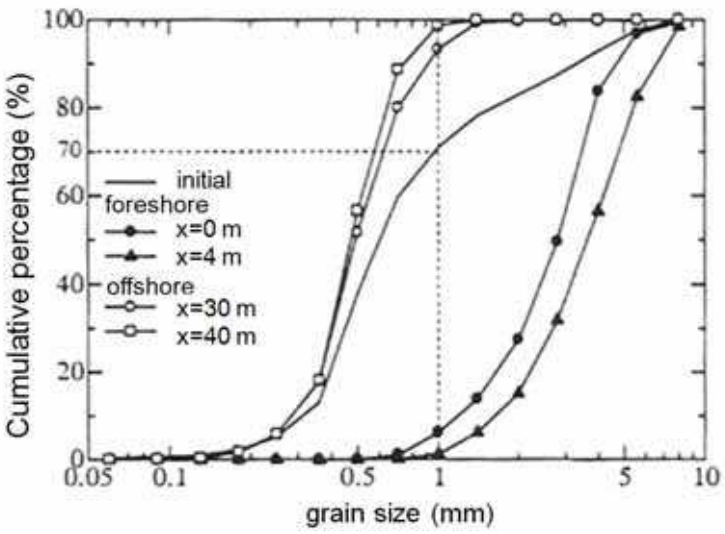

Fig. 4. Cumulative grain size distributions on foreshore and offshore beds in experiment

Figure 4 shows the cumulative grain size distributions on the foreshore and offshore beds. The grains in the foreshore and offshore zones are clearly separated into two grain size populations of grain sizes larger and smaller than 1 mm, respectively. On the basis of this result, hereafter, we simply refer to the grain size population with grain size smaller than 1 mm as fine sand and that with grain size larger than 1 mm as coarse sand. The experimental results are summarized as follows.

a. Erosion occurred only in a zone shallower than the depth of closure h_c=1.3 m.
b. Coarse sand was transported shoreward, forming a 0.5-m-high berm and a foreshore with a slope of 1/6.
c. The volume of coarse sand contained in the erosion zone is limited, and the development of a berm depends on this volume of coarse sand. Although the berm height depends on the wave characteristics, a minimum volume of coarse sand is required for the development of a berm.
d. Fine sand was transported to a zone deeper than h_c, and a slope of 1/10, which was larger than the initial slope, was formed on the offshore bed.
e. After a berm was sufficiently developed, the beach profile became stable, because the grain size on the foreshore matched the slope. The offshore flat bed near h_c also became stable because further erosion did not occur, resulting in the cessation of the offshore discharge of fine sand. Thus, the equilibrium condition is assumed to form only when a berm is sufficiently developed.

3.2 Calculation conditions for application to experimental results

As calculation conditions, two grain size populations with only grain sizes of $d^{(1)}$=0.45 mm and $d^{(2)}$=3 mm, which represent typical fine and coarse sands, respectively, and with no

overlap of the grain size distribution were assumed, because grain sorting occurred at a critical grain size of 1 mm in the experiment. These grain sizes were determined on the basis of the cumulative grain size distribution of the sand of mixed grain sizes used in the experiment; thus, $d^{(1)}$ and $d^{(2)}$ were approximately equal to d_{50} calculated from all the fine and coarse sand samples, respectively, and the mean grain size of all the samples d_m used in the experiment became equal to 1.21 mm.

Cases	Reproduction: $\mu^{(1)}=0.7$ and $\mu^{(2)}=0.3$ Prediction: Case 1: $\mu^{(1)}=0.1$ and $\mu^{(2)}=0.9$ Case 2: $\mu^{(1)}=0.3$ and $\mu^{(2)}=0.7$ Case 3: $\mu^{(1)}=0.5$ and $\mu^{(2)}=0.5$ Case 4: $\mu^{(1)}=0.9$ and $\mu^{(2)}=0.1$
Initial topography	Uniform slope of $\tan\beta=1/20$
Grain size	Number of grain sizes: N=2 Fine sand $d^{(1)}=0.45$ mm, Coarse sand $d^{(2)}=3$ mm Initial content $\mu^{(1)}=0.7$ and $\mu^{(2)}=0.3$
Width of exchange layer	B=0.4 m
Wave conditions	Breaker height: $H_b=0.75$ m ($H_0=0.6$ m, T=3.5 s) Breaker angle: $\alpha_{bs}=0$ deg. Tide level: mean sea level
Depth of closure	$h_c=1.3$ m
Berm height	$h_R=0.5$ m
Coefficients of sand transport	A=0.2 and $\gamma=1.0$
Depth distribution of sand transport rate	Cubic equation given by Uda and Kawano (1996)
Equilibrium slope	$\tan\beta_c^{(1)}=1/100$ (fine sand) $\tan\beta_c^{(2)}=1/6$ (coarse sand)
Critical slope	Fine sand: 1/2 on land and 1/10 on seabed Coarse sand: 1/2 on land and 1/3 on seabed
Calculation domain	z=+1.0 m to -3.0 m
Mesh size	$\Delta z=0.1$ m
Time interval	$\Delta t=0.01$ h
Total time of calculation	t=200 h (20,000 steps)
Boundary conditions	$q_z=0$ at landward and offshore boundaries
Calculation method	Explicit finite difference method

Table 1. Calculation conditions

The initial content of sand was assumed to be $\mu^{(1)}$=0.7 for fine sand and $\mu^{(2)}$=0.3 for coarse sand, the same condition as that in the experiment. The initial beach profile is given a uniform slope of 1/20, and h_R and h_c are set as h_R=0.5 m and h_c=1.3 m, on the basis of the experimental results. As equilibrium slopes, the gentle seabed slope composed of fine sand in the offshore zone and the steep seabed slope composed of coarse sand are given as $tan\beta_c^{(1)}$=1/100 and $tan\beta_c^{(2)}$=1/6, respectively, with reference to the experimental results. The width B of the exchange layer is given by the thickness of the exchange layer divided by the slope. The thickness of the exchange layer is given as 0.02 m, which is 3% of the breaker height (H_b =0.75 m), on the basis of the results obtained from the field observation by Kraus (1985), and B is set to be 0.4 m, obtained by dividing the exchange-layer thickness by the initial slope of 1/20.

The critical slope of sinking for sand of each grain size is separately set on land and on the seabed, similarly to that in the work of Uda et al. (2004). In this study, the sinking of fine sand into the zone deeper than h_c is considered to be caused by gravity and the critical slope is given by a slope of 1/10, which occurred in the experiment. In the other zone, the critical slopes are set to be 1/2 and 1/3 on land and on the seabed, respectively, as indicated by Uda et al. (2004).

The coefficient of sediment transport A, which defines the rate of beach change, was determined as A=0.2 by a trial calculation, so that the numerical simulation can reproduce the development of a berm in 20 hours as in the case of the experiment. For the depth distribution of cross-shore sand transport, the same depth distribution of longshore sand transport as that in Eq. (6) given by Uda and Kawano (1996) was assumed. As the wave condition, the time-averaged breaker height taken from the observation results, H_b=0.75 m, was used. Other calculation conditions, such as mesh size and time step, are shown in Table 1.

3.3 Results

3.3.1 Comparison with experimental results

First, numerical simulation was carried out under the same conditions as those of the experiment. Figure 5 shows the change in the longitudinal profile with time for the contents of fine and coarse sand of $\mu^{(1)}$=0.7 and $\mu^{(2)}$=0.3, respectively. Erosion starts from a shallow zone near the shoreline, and part of the sand is transported landward, forming a berm on the foreshore. Sand is also transported offshore, forming a small hump in the offshore zone. Figure 6 shows the measured and predicted longitudinal profiles after wave action. The results are in good agreement in terms of the formation of a berm and the flat offshore sea bottom and offshore depositions of sand. Figures 7(a) and 7(b) show the cross-shore distributions of the contents $\mu^{(1)}$ and $\mu^{(2)}$ corresponding to the profile changes shown in Fig. 5. The foreshore materials become only coarse sand ($\mu^{(1)}$=0, $\mu^{(2)}$=1.0), whereas the offshore seabed with a gentle slope becomes covered with only fine sand ($\mu^{(1)}$=1.0, $\mu^{(2)}$=0). As a result, the cross-shore distribution of the mean grain size shown in Fig. 8 is obtained. The grain size is large at 3.0 mm on the steep slope of the foreshore and on the berm, whereas on the offshore seabed, it becomes as small as 0.5 mm. These results correspond well to the cross-shore distribution of d_{50}, as shown in Fig. 3.

In conclusion, the changes in the longitudinal profile in the experiment were accurately reproduced in the numerical model. It was found that fine and coarse sands are sorted on model beaches composed of sand of mixed grain size, and that coarse and fine sands are transported shoreward and offshore, respectively, finally approaching the equilibrium slope corresponding to each grain size population.

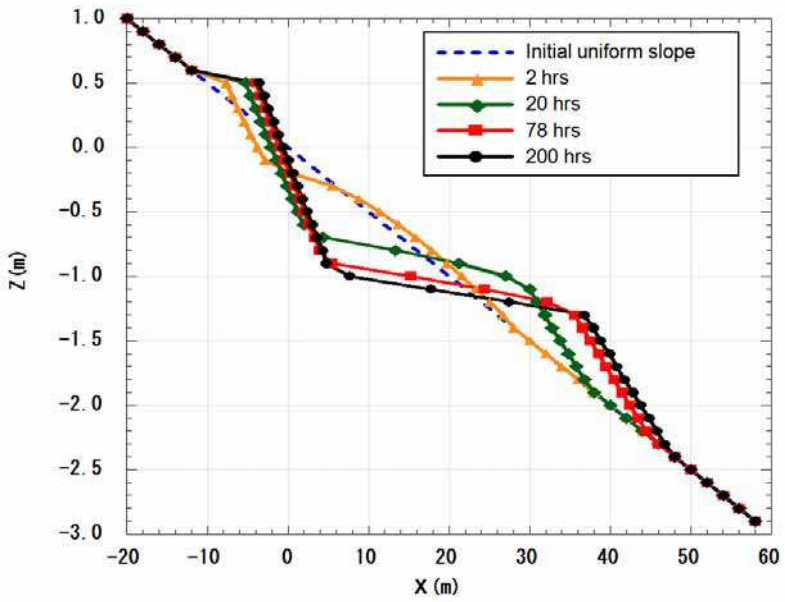

Fig. 5. Change in longitudinal profile with time for contents of fine and coarse sand of $\mu^{(1)}$=0.7 and $\mu^{(2)}$=0.3, respectively

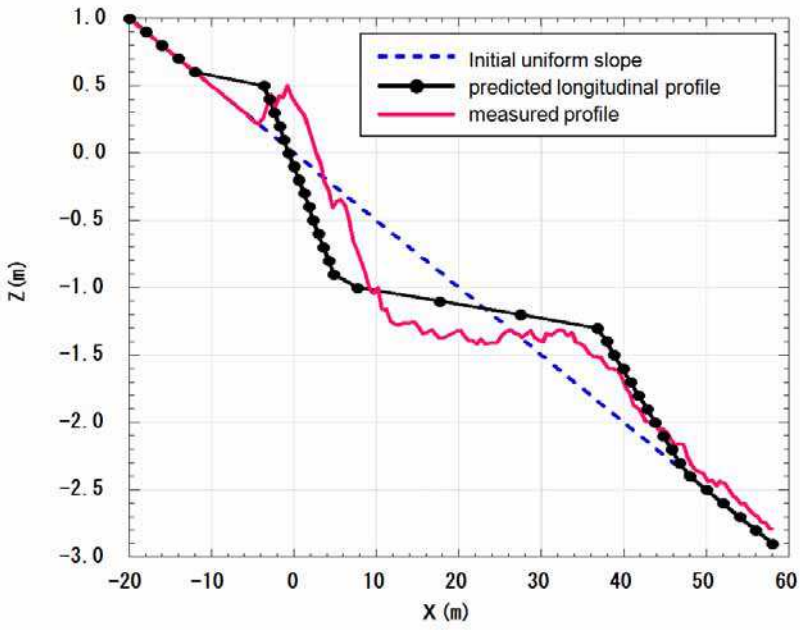

Fig. 6. Measured and predicted longitudinal profiles after wave action

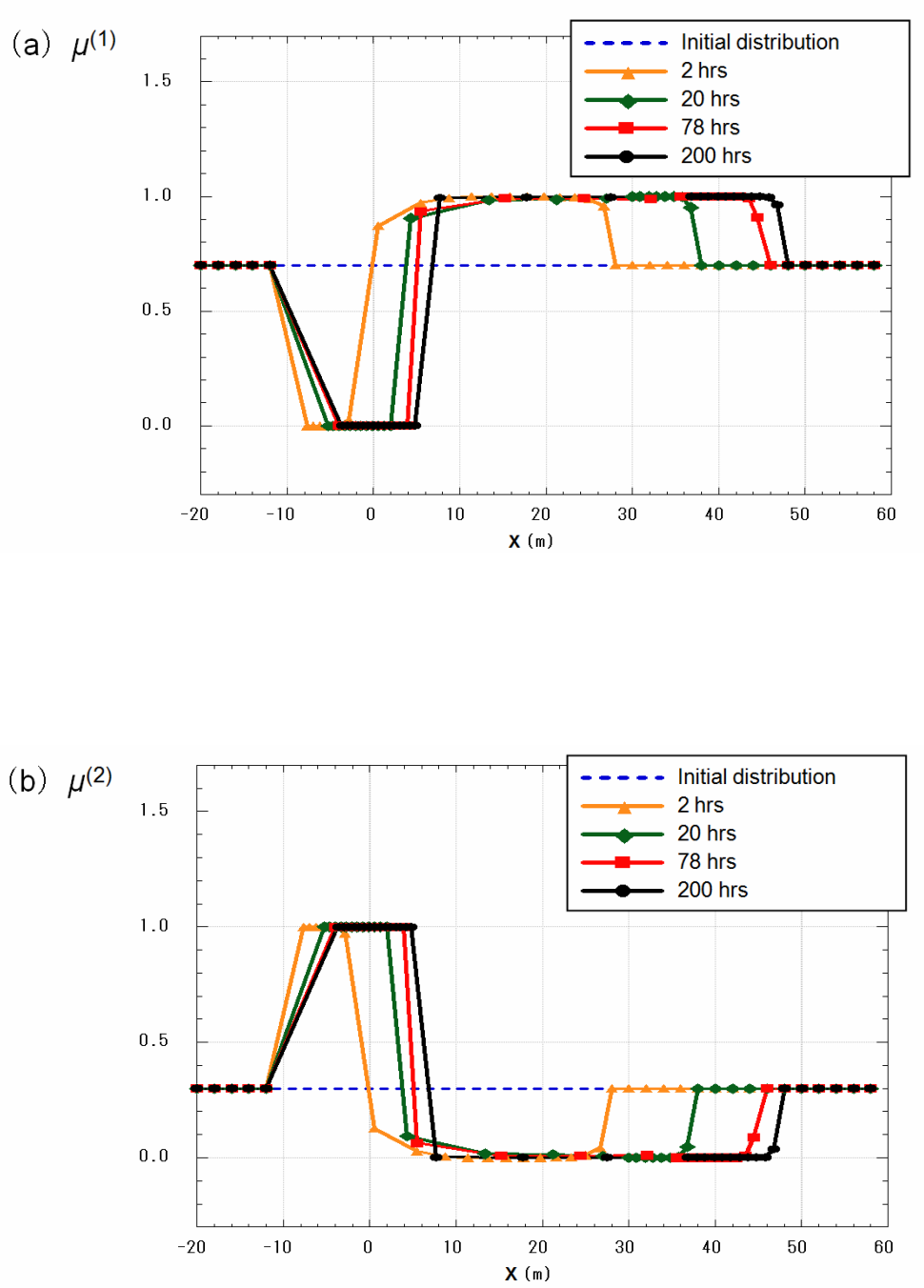

Fig. 7. Cross-shore distributions of contents $\mu^{(1)}$ and $\mu^{(2)}$ of fine and coarse sand, respectively

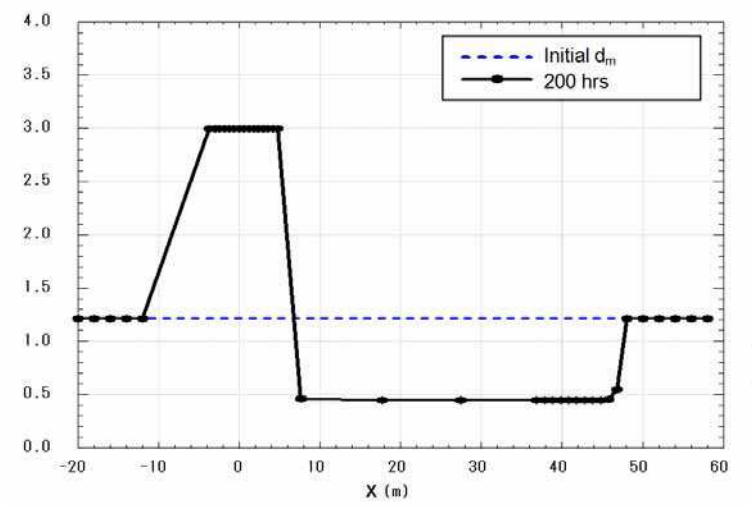

Fig. 8. Cross-shore distribution of mean grain size

3.3.2 Changes in initial content and equilibrium profile

The effect of the difference in the initial contents on the final, stable profile can be investigated, assuming the initial contents of fine and coarse sand are $\mu^{(1)}$=0.3 and $\mu^{(2)}$=0.7, respectively. Figure 9 shows the results. As a result of the increase in the content of coarse sand, the volume of sand transported shoreward increased compared with that in the case shown in Fig. 5, and a berm predominantly developed. In contrast, a smaller volume of sand was transported offshore.

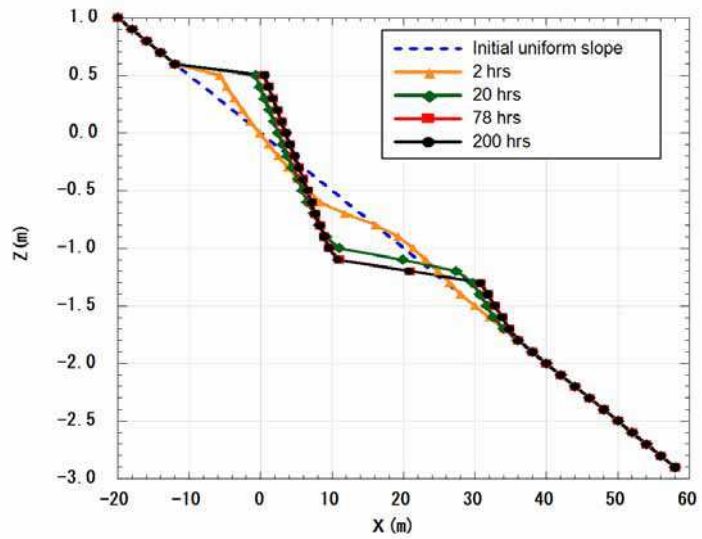

Fig. 9. Predicted changes in longitudinal profile when $\mu^{(1)}$ and $\mu^{(2)}$ are 0.3 and 0.7, respectively

Figure 10 shows the final, stable profiles in the cases where the initial contents ($\mu^{(1)}$, $\mu^{(2)}$) were altered to (0.9, 0.1), (0.5, 0.5), (0.3, 0.7) and (0.1, 0.9), as well as the result of the reproduction case with (0.7, 0.3). A larger berm develops with the increase in the content of coarse sand, $\mu^{(2)}$. In contrast, a smaller berm develops with the increase in the content of fine sand, $\mu^{(1)}$, and offshore sand transport becomes dominant, accelerating the deposition of fine sand in the offshore zone. Thus, the grain size has a marked effect on the changes in the longitudinal profile. On a beach composed of only fine sand, offshore sand transport from the initial stage never converges and an equilibrium profile cannot be attained. The equilibrium profile is formed in the wave flume experiment only when a sufficient volume of coarse sand is available to cover the foreshore and to form a berm.

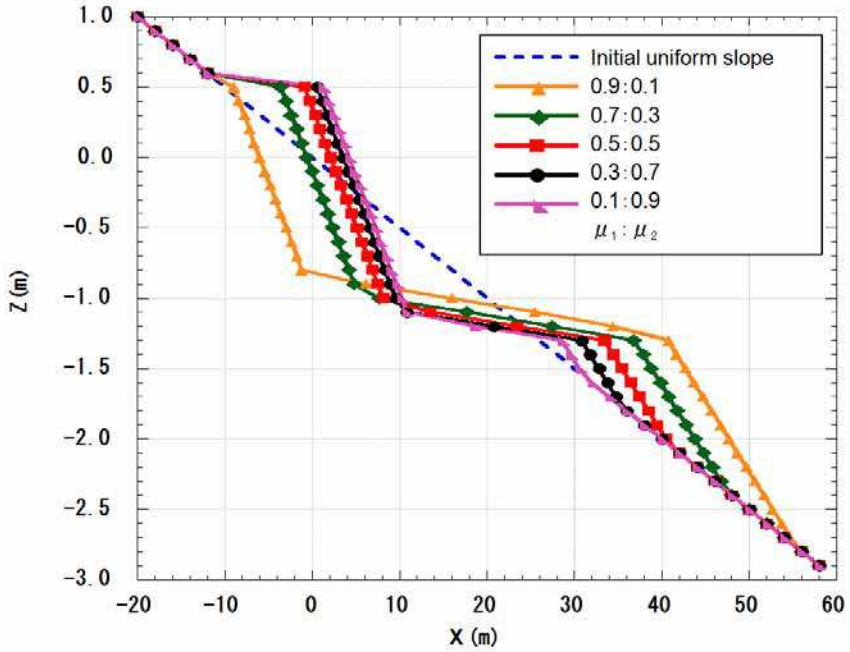

Fig. 10. Final, stable profiles in cases where initial contents ($\mu^{(1)}$, $\mu^{(2)}$) are altered to (0.9, 0.1), (0.5, 0.5), (0.3, 0.7) and (0.1, 0.9), as well as result of reproduction case with (0.7, 0.3)

4. Application of model to prediction of beach changes after nourishment at Chigasaki coast

4.1 General conditions of Chigasaki coast

On the Chigasaki coast, which is located in Sagami Bay in Japan, beach erosion has been severe. The main causes of beach erosion are the decrease in fluvial sand supply from the Sagami River, triggered by the construction of several dams in the upstream basin, and the obstruction of longshore sand transport by the Chigasaki fishing port, located east of the river mouth (Fig. 11). As a measure against beach erosion, an artificial headland was built in 1991 and beach nourishment has been carried out since 1991. To significantly improve the coastal conditions, beach nourishment at a rate of 3×10^4 m^3/yr has been planned with the

aim of recovering the foreshore to a width of 50 m downcoast of the fishing port. The numerical model was used for studying the difference in the response of nourishment sand of different grain sizes (Yoshioka et al., 2008).

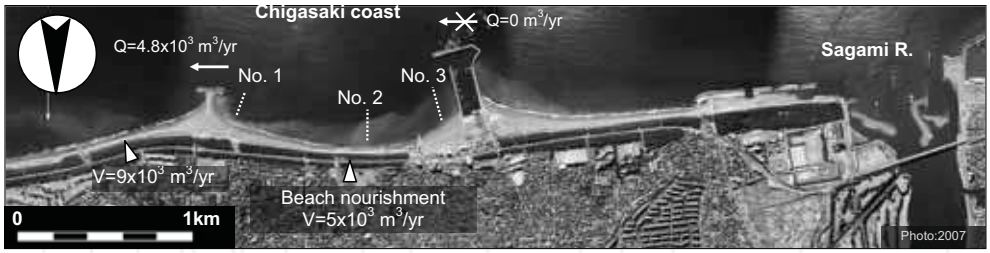

Fig. 11. Aerial photograph of Chigasaki coast and alignment of transects

4.2 Calculation conditions

Figure 11 shows the calculation domain of the Chigasaki coast along with the alignment of transects. A Cartesian coordinate system is used. The bathymetric changes between 1991 and 2005 after the construction of the artificial headland were reproduced. Then, the topographic and grain size changes after 10 years were predicted for beach nourishment using sand of different grain sizes. Regarding beach nourishment, the same volume of sand as that used for annual nourishment was supplied at two locations, and the same amount of sand was extracted from the downcoast boundary of the calculation domain.

Figure 12 shows the depth distribution of d_{50} of all the seabed materials sampled, the grain size populations of which are separated into the following three categories: fine sand in a zone deeper than -5 m, medium and coarse sand between -5 m and the land, and gravel near the shoreline.

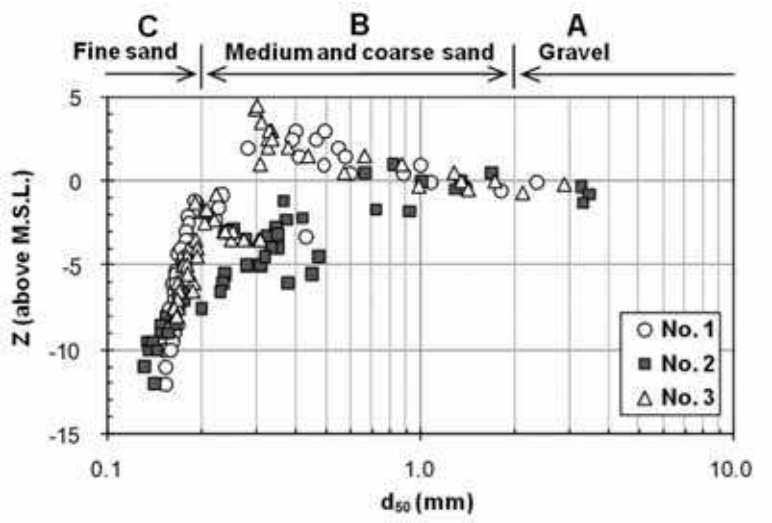

Fig. 12. Depth distribution of d_{50}

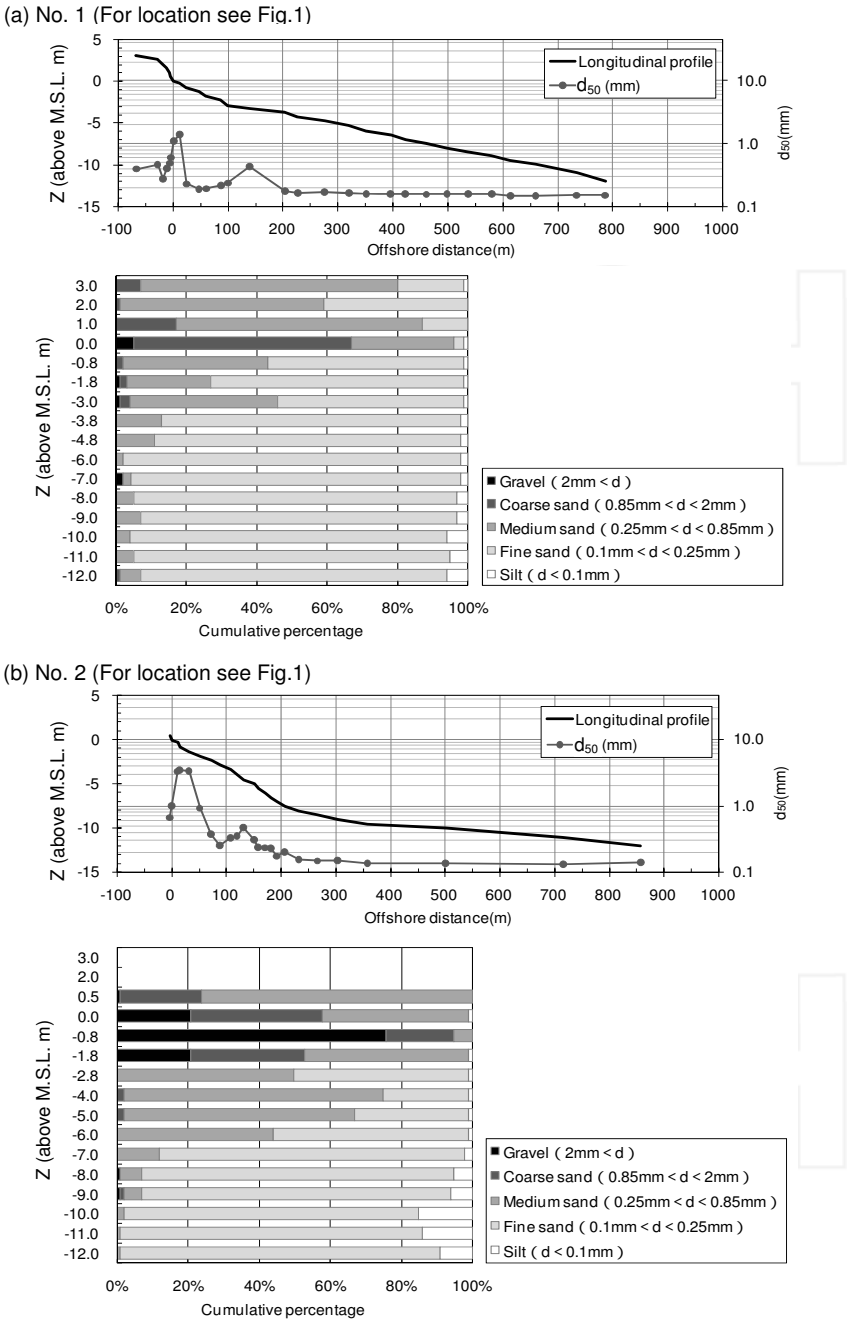

Fig. 13. Longitudinal profiles, cross-shore distributions of d_{50} and contents of grain sizes of bed materials along transect Nos. 1 and 2

Coordinate system	Cartesian coordinates considering actual seabed topography
Initial topography	Parallel, straight contour lines
Wave conditions	Energy-mean waves, H_b=0.83 m, T=6.4 s, and wave direction=S6°W
Water level	Mean sea level
Depth of closure, h_c and berm height, h_R	h_c =9 m and h_R =3 m
Grain size conditions	Grain size populations: Grain size 1: fine sand (d_{50}=0.15 mm) Grain size 2: coarse and medium sand (d_{50}=0.20 mm) Grain size 3: gravel (d_{50}=2.0 mm)
	Equilibrium slope and thickness of exchange layer: Grain size 1: 1/80 and 0.625 m Grain size 2: 1/30 and 1.667 m Grain size 3: 1/10 and 5 m
	Contents for reproduction calculation: μ_1=0.48 (grain size 1) μ_2=0.39 (grain size 2) μ_3=0.13 (grain size 3)
	Contents for prediction: μ_1=0.48, μ_2=0.39, μ_3=0.13 (for present materials) μ_1=0.10, μ_2=0.23, μ_3=0.67 (for coarse materials) μ_1=0.90, μ_2=0.05, μ_3=0.05 (for fine materials)
Coefficients of sand transport	Coefficient of longshore sand transport: $K_x=0.387/\sqrt{d_{50}}$ Grain size 1: K_x=0.1000 Grain size 2: K_x=0.0866 Grain size 3: K_x=0.0274 Coefficient of cross-shore sand transport: $K_z=0.4K_x$ Ozasa and Brampton coefficient: $K_2=1.62K_z$
Depth distribution of sand transport rate	Cubic equation given by Uda and Kawano (1996)
Critical slopes for sinking of sand	1/2 on land and 1/3 on seabed
Calculation domain	z=+3 m to -9 m
Mesh size	ΔX=100 m and Δz=1 m
Time interval	Δt=50 h, 180 steps /yr
Calculation period	From 1991 for reproduction and 10 years for prediction
Boundary conditions	Right boundary: reproduction Q_{in}=0 m^3/yr Left boundary: $Q_{out}=1.4x10^4$ m^3/yr Landward and offshore boundaries: q_z=0
Calculation method	Explicit finite difference method

Table 2. Calculation conditions

Figure 13 shows the longitudinal profiles and cross-shore distributions of d_{50} along transect Nos. 1 and 2 located near the headland and in the eroded zone, respectively, as shown in Fig. 11, as well as the cumulative percentage of grain sizes at certain depths. It is clear that the beach material is mainly composed of fine sand (d=0.1-0.25 mm) and medium and coarse sand (d=0.25-2 mm). In addition, gravel appears in a depth zone between the shoreline and 1 m depth. Taking these characteristics into account, the following three grain size populations are required in the numerical simulation: population 1 sand with a grain size smaller than 0.2 mm; population 2 medium and coarse sand (d=0.2-2 mm); and population 3 gravel (d>2 mm). Furthermore, the equilibrium slopes corresponding to these grain size populations are 1/80, 1/30 and 1/10, respectively, on the basis of the mean longitudinal slopes in the depth zone where each grain size population is dominant, as shown in Fig. 13.

In the reproduction calculation, the contents of the three grain size populations were determined from the observed data shown in Fig. 13, by taking the weighted average as a function of the seabed length. In the prediction, the contents of the three grain size populations (fine sand, medium and coarse sand, and gravel) were assumed to be 0.10:0.23:0.67 for coarse materials and 0.90:0.05:0.05 for fine materials on the basis of the materials to be used for nourishment, as well as the content of the present materials on the coast. The other calculation conditions are shown in Table 2. For incident waves, the energy-mean significant wave height of this coast (H_b=0.83 m and T=6.4 s) is used. The wave direction is determined by a trial-and-error method so as to obtain the best-fit result. The depth range in which beach changes occur is between the berm height h_R=3 m and the depth of closure h_c=9 m as revealed by the measured bathymetric changes. The wave diffraction due to the existence of the offshore reef and Chigasaki fishing port was calculated by the angular spreading method for irregular waves (Sakai et al., 2006).

4.3 Results of reproduction calculation

The beach changes between 1991, when the artificial headland was constructed, and 2005 were reproduced by numerical simulation. On the coast, beach nourishment to maintain the beach has been carried out since 1991, and a dynamically stable beach has now been formed without large changes in the shoreline position or beach topography. This dynamically stable beach topography was reproduced by the numerical calculation. Figure 14 shows the contours predicted under the dynamically stable condition, in which 5,000 and 9,000 m^3 of sand with the same contents of the three grain size populations as those measured on the present coast were supplied from two locations in the domain, and the same amount of sand was extracted from the left boundary. The measured shoreline configuration is also shown.

The predicted and measured shoreline configurations are in good agreement. This dynamically stable condition was reproduced by supplying sand at the rate of 5,000 m^3/yr to the Chigasaki coast, which approximately agrees with the average rate of past beach nourishment of 4,800 m^3/yr. Furthermore, the meandering of the contour lines deeper than 5 m off the artificial headland, and the concave profile, which changes from a steep slope near the shoreline to a gentle slope in the offshore zone, as shown in Fig. 13, were also reproduced in Fig. 14.

Figure 15 shows the predicted longitudinal profile and cross-shore mean grain size distribution. These results are in agreement with the measured values, as shown in Fig. 13(a), along the centerline of the pocket beach, by superimposing the shoreline position at Y=580 m in Fig. 15 with that at Y=0 m in Fig. 13(a). Gravel with a grain size larger than 2

mm is concentrated on the foreshore with an elevation higher than +1 m, the zone between the shoreline and 3 m depth is covered with fine sand with a grain size of 0.2 mm, and the seabed further offshore is covered with fine sand with a grain size of 0.15 mm. Thus, grain size sorting, from the coarse sand mainly composed of gravel on the foreshore to the offshore bed covered with fine sand, is well reproduced.

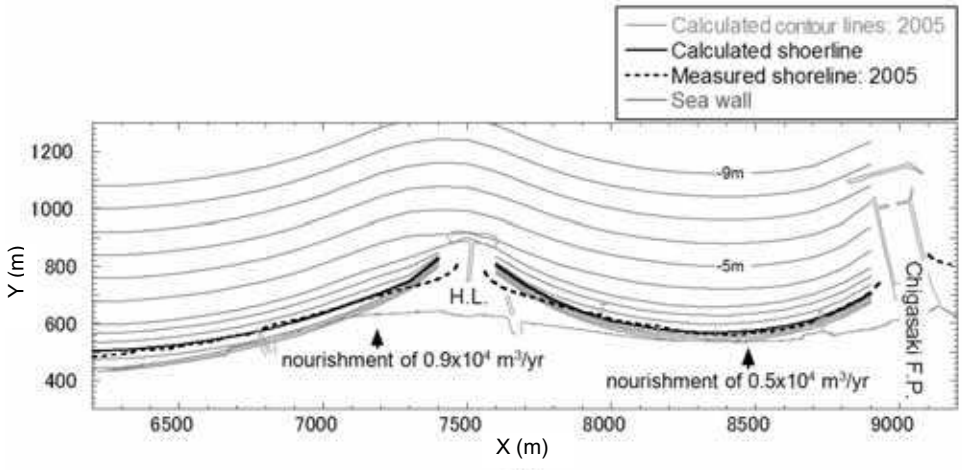

Fig. 14. Reproduced contour lines and comparison of measured and predicted shoreline configurations

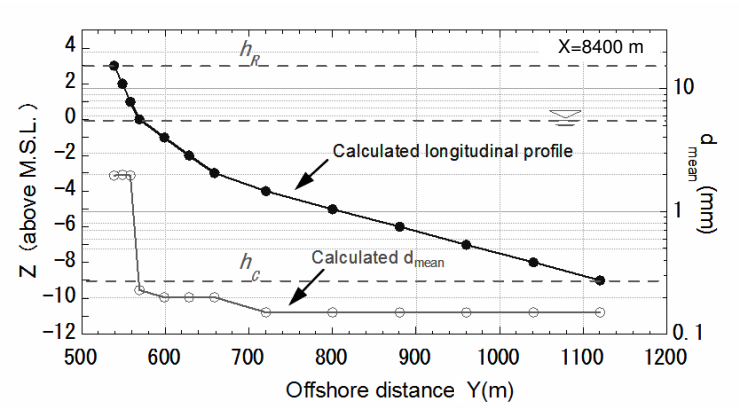

Fig. 15. Predicted longitudinal profile and cross-shore distribution of mean grain size

4.4 Further applications

By setting the minimum width of the beach to be nourished as 50 m, topographic and grain size changes after 10 years were predicted with several types of materials composed of grains with different sizes being used for beach nourishment. The nourishment site is located between X=8.4 and X=8.6 km, and the materials used for nourishment were supplied

from a berm on the shore face between the shoreline and 3 m height. The sand supply is assumed to be 3.0×10^4 m^3/yr in accordance with the planned nourishment.

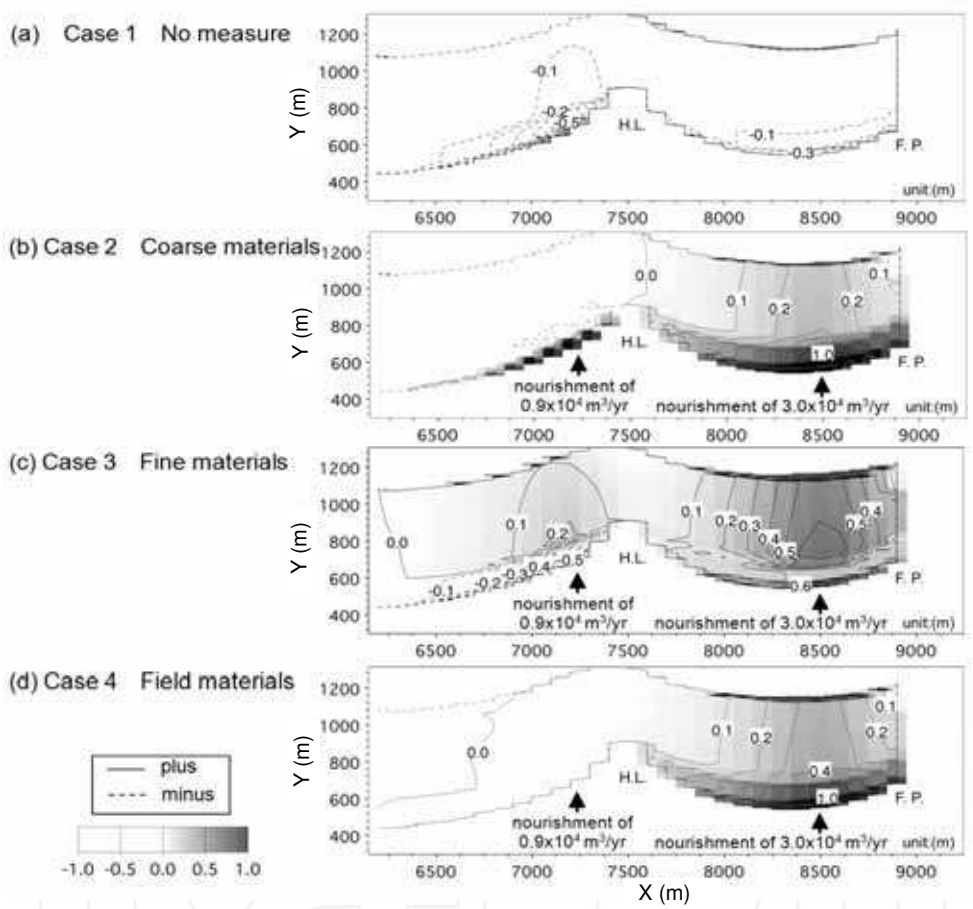

Fig. 16. Bathymetric changes relative to initial beach topography in four cases

Figures 16 and 17 show the planar distribution of the change in depth and the shoreline changes from the initial seabed topography in the following four cases: no nourishment (case 1), nourishment using coarse sand (case 2), nourishment using fine sand (case 3), and nourishment using sand with the same mean grain size as that of the current beach (case 4). When the beach receives no nourishment, further erosion occurs on the Chigasaki coast and east of the artificial headland, resulting in shoreline recession (Figs. 16(a) and 17(a)). For beach nourishment using coarse sand, the seabed level increases over an extensive area including the offshore zone, sand deposition is concentrated near the shoreline (Fig. 16(b)) and the shoreline markedly advances by up to 35 m, approaching the level of the shoreline in 1954 (Fig. 17(b)). Thus, beach nourishment using coarse sand is effective for protecting the shoreline.

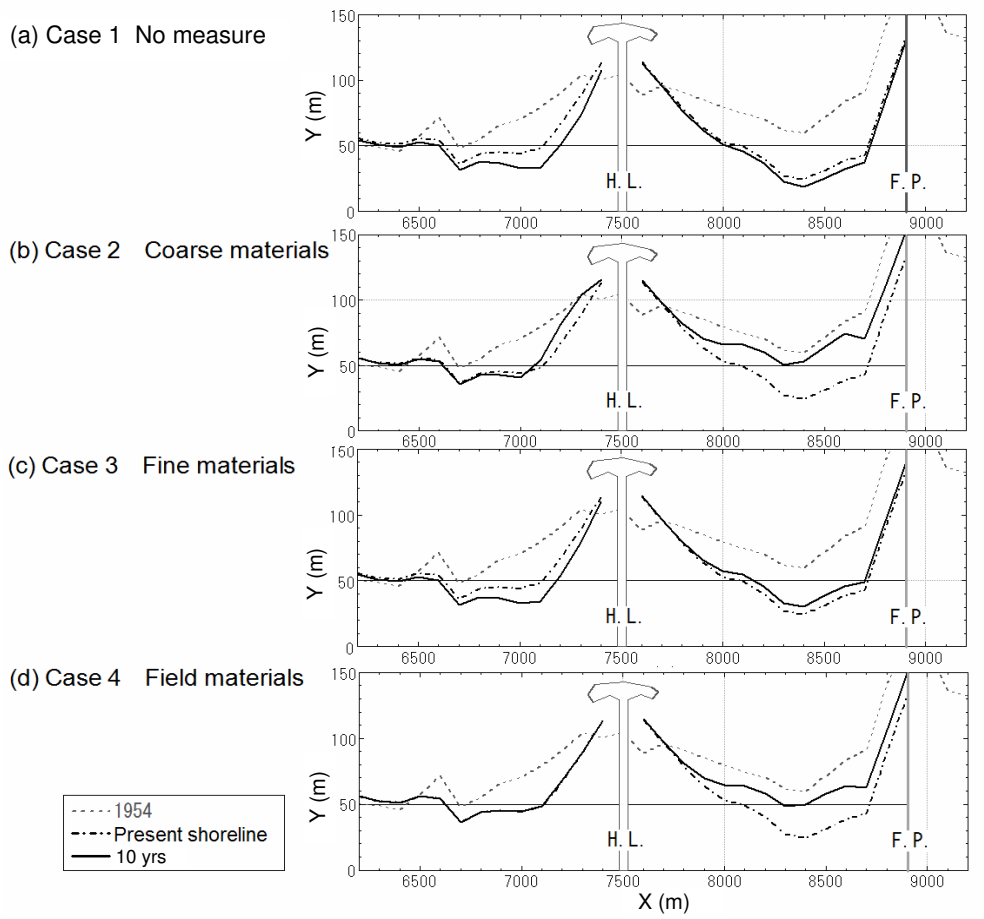

Fig. 17. Shoreline changes in four cases

For beach nourishment using fine sand, the nourishment sand is mainly diffused offshore without being deposited near the shoreline, which is different from the case of nourishment using coarse sand (Fig. 16(c)). The increase in the seabed elevation over an extensive offshore zone is greater than that in the case of nourishment using coarse sand. In contrast, the shoreline advance is much less that that in the case of nourishment using coarse sand (Fig. 17(c)). Furthermore, the beach was further eroded east of the artificial headland, despite the beach nourishment west of the headland. For beach nourishment using sand with the same mean grain size as that of the beach, a significant nourishment effect was predicted, although this effect was less than that of beach nourishment using coarse sand (Fig. 16(d)), and a significant shoreline advance was predicted, as shown in Fig. 17(d).

Figure 18 shows the changes in the longitudinal profile and cross-shore mean grain size distribution along transect X=8.4 km. When the beach receives no nourishment, a concave profile and the accumulation of coarse materials on the foreshore were predicted, as shown in Fig. 18(a), which are in good agreement with the measured results shown in Fig. 13. For

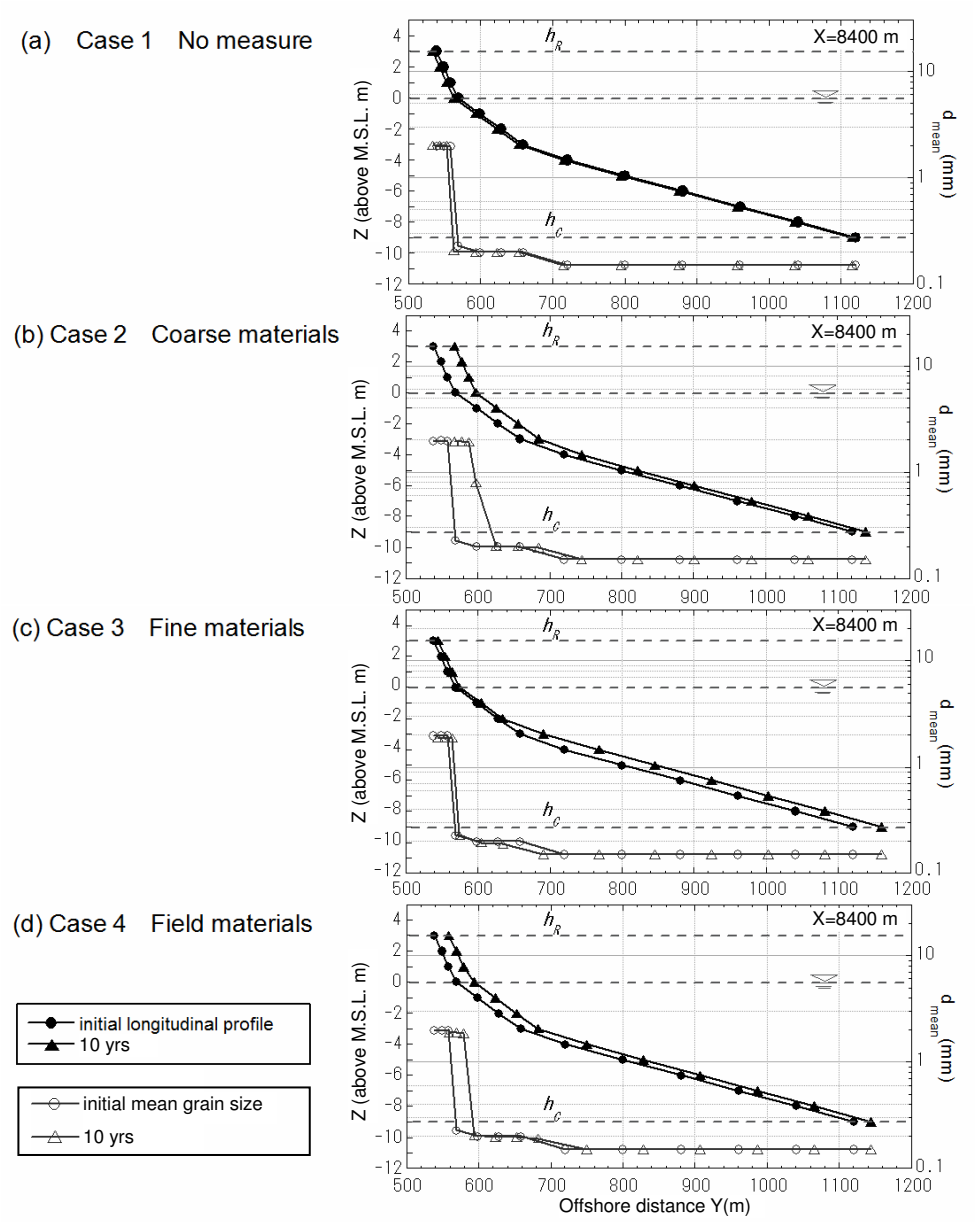

Fig. 18. Changes in longitudinal profile and mean grain size along centerline of pocket beach

beach nourishment using coarse sand, the longitudinal profile generally moves offshore, and the bed materials in the zone where the longitudinal profile markedly moves offshore are mainly composed of sand with a grain size of 2 mm (Fig. 18(b)). In the case of beach

nourishment using fine sand, the change in the longitudinal profile shows that the shoreline advance is minimal, and the fine sand is transported offshore by its seaward movement and covers the offshore seabed (Fig. 18(c)). For beach nourishment using coarse sand and sand with the same mean grain size as that of the beach, coarse materials are selectively deposited near the shoreline. Finally, it is concluded that an excellent shore protection effect can be expected by beach nourishment using coarse sand or sand with the same mean grain size as that of the beach, whereas fine nourishment sand is widely diffused offshore, although beach nourishment using materials containing a large amount of fine sand is preferable for increasing the offshore seabed elevation.

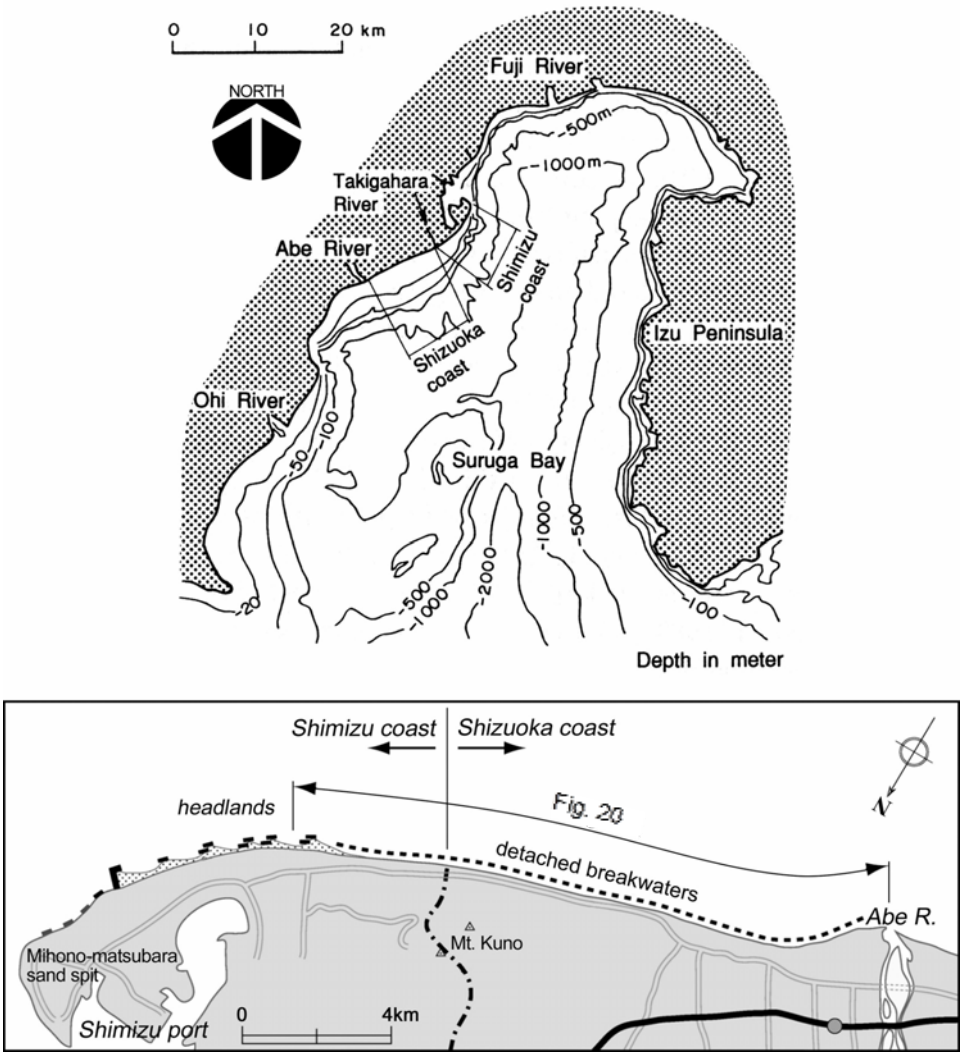

Fig. 19. Location of Shimizu coast

5. Application of model to prediction of beach changes on Shimizu coast

5.1 General conditions of Shimizu coast

Beach erosion has been severe on the Shimizu coast, which extends along the outer marginal coastline of the Mihono-Matsubara sand spit in Suruga Bay, as shown in Fig. 19, because of the decrease in longshore sand supply from the Abe River. As a measure against beach erosion, five sets of artificial headlands and an L-shaped groin were constructed between 1989 and 1999 (Uda et al., 2007). At present, the shoreline of this coast is barely maintained by these facilities and beach nourishment, and large topographic changes have been observed around these structures. Bathymetric surveys and bottom sampling have been carried out over an extensive area to investigate the mechanism of these beach changes. The analysis of the data sets suggests that there are two "conveyer belts" carrying gravel and fine sand along the coastline, and that these conveyer belts have been deformed as a result of the construction of the coastal structures. Here, the mechanism of the development and deformation of these conveyer belts is investigated using the present model (Nishitani et al., 2008).

5.2 Bathymetric changes, grain size distribution and shoreline changes

Figure 20 shows the bathymetry of the study area in March 2006. The transects of sea bottom sounding are arranged at 100 m intervals from the north end of the study area. Headland (HL) No. 1 is located at transect No. 65 at the south end of the study area, and the L-shaped groin (L-groin) is located at transect No. 32. In the study area, the contours in the zone deeper than 5 m smoothly extend alongshore, whereas those in the zone shallower than 5 m advance (retreat) south (north) of each headland because of their effect of blocking longshore sand transport. A submarine canyon with a very steep slope develops to the north of the L-groin.

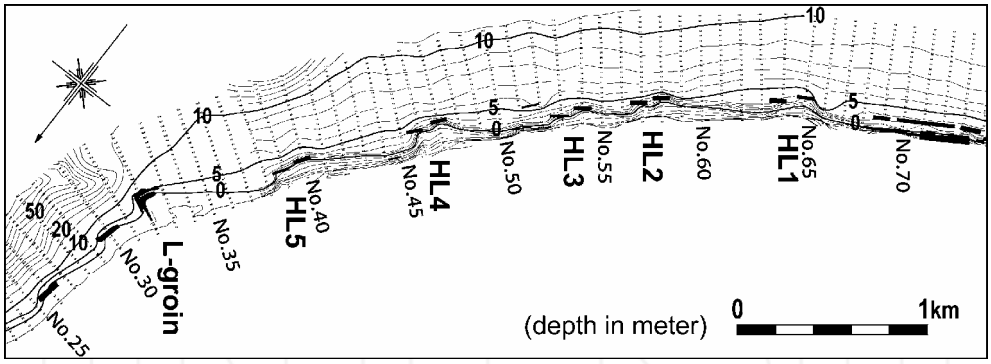

Fig. 20. Bathymetry of Shimizu coast and alignment of transects

Figure 21 shows the shoreline changes relative to the shoreline position in 1989 immediately before the construction of the artificial headlands. Since northward longshore sand transport prevails in the study area, the shoreline retreated downcoast of the headlands, which were successively constructed over time, resulting in a step-type coastline. The longitudinal profiles and depth changes in the median diameter d_{50} determined from the bottom sampling carried out in August 2006 were compared along several transects where typical shoreline changes were observed, as shown in Fig. 22.

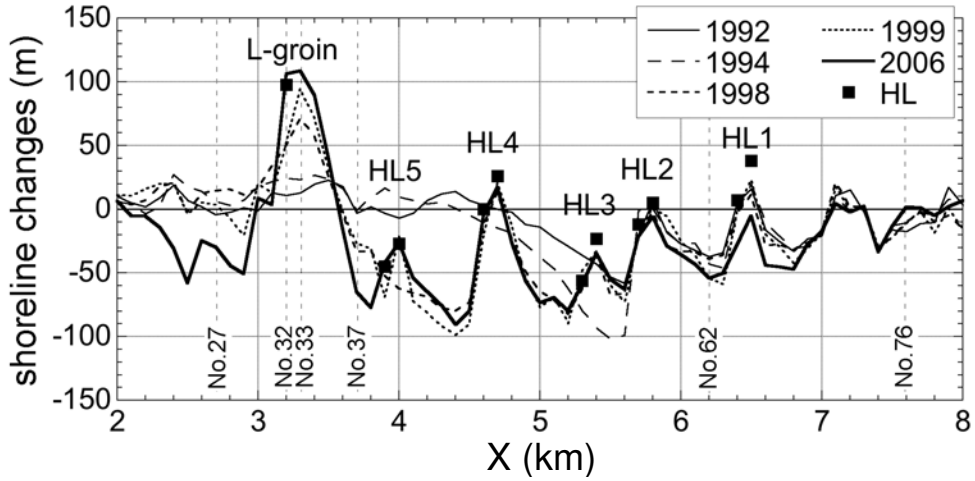

Fig. 21. Shoreline changes with reference to shoreline in 1989

Along transect No. 76, located at the south end of the study area, beach erosion occurred in the early years, but no large shoreline changes were observed, even in the comparison of the shoreline positions in 1989 and 2006 (Fig. 22(a)). A concave profile was formed with a steep slope of 1/10 from the foreshore to 4 m depth and a gentle offshore slope in the depth zone greater than 4 m. Corresponding to these slope changes, the foreshore is covered with gravel with median diameter d_{50} ranging between 10 and 30 mm, whereas d_{50} becomes as small as 0.18 mm in the depth zone between 4 and 7 m, and 0.16 mm in the zone deeper than 9 m. In particular, note that the offshore seabed with a slope of 1/50 at depths between 5 and 8 m is covered with fine sand.

Along transect No. 62, located downcoast of HL No. 1 where the shoreline significantly retreated between 1989 and 1992, we observed a steep slope mainly covered with gravel in the zone shallower than 2 m and with fine sand in the zone between 2 and 5 m. This slope was eroded, resulting in the parallel landward movement of the profile (Fig. 22(b)). In contrast, the seabed changes are negligible in the zone deeper than 5 m, where the seabed is covered with fine sand with d_{50}=0.16 mm.

Along transect No. 37, located downcoast of HL No. 5, the shoreline receded after the construction of HL No. 5 (Fig. 22(c)). A convex profile had formed before the erosion, but a profile change from convex to concave occurred because of beach erosion, and the seabed shallower than 4 m depth was significantly eroded. In contrast, sand was deposited in the zone between 4 and 7 m deep, and d_{50} for the sand deposited in this zone is 0.16 mm. Thus, the selective deposition of fine sand in the offshore zone deeper than 4 m is in marked contrast to that of gravel near the shoreline.

Along transect No. 33 located 200 m south of the L-groin (Fig. 22(d)), the shoreline advanced by as much as 100 m between 1989 and 2006 with a parallel movement of the longitudinal profile. Major beach changes were observed up to a depth of 9 m, which is greater than the critical depth observed along the other transects. Note that gravel is deposited in the zone shallower than 3 m, whereas fine sand with d_{50}=0.16 mm covers the seabed in the zone between 3 and 10 m deep; d_{50} increases with the depth of the seabed in the zone deeper than 10 m. This is a special characteristic only observed along this transect.

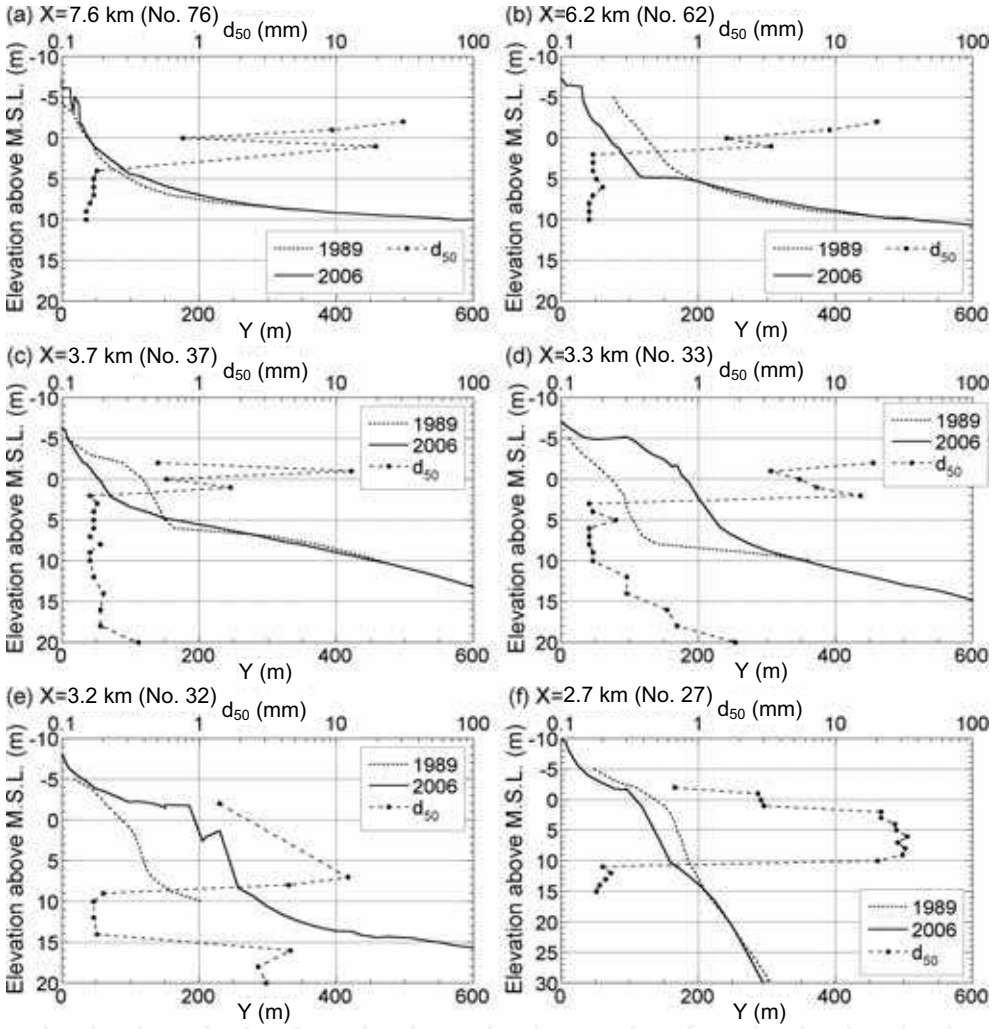

Fig. 22. Changes in longitudinal profile and depth distribution of d_{50}

Along transect No. 32 located upcoast of the L-groin, the shoreline advanced by 110 m between 1989 and 2006, as shown in Fig. 22(e), because of the blockage of longshore sand transport by the L-groin, and the longitudinal profile between +2 and -8 m moved parallel with the shoreline advance. The profile in 1989 can be smoothly connected to the profile in 2006 by extrapolation, since a very gentle slope extends in the zone at a depth greater than 8 m. In contrast, the longitudinal profile in 2006 has a break at a depth of 8 m, and the seabed slope becomes gentle at this depth. Comparing the depth distribution of d_{50} and the profile in 2006, we found that d_{50} ranges between 1.4 and 12 mm, and gravel mainly accumulates in the zone shallower than 9 m, whereas the offshore seabed between 9 and 14 m is covered with fine sand with d_{50}=0.16 mm, and then a gravel bed appears at depths greater than 14 m. Major beach changes can be observed up to a depth of 8 m, but the deposition of fine

sand with d_{50} =0.16 mm also takes place in the zone at depths between 8 and 10 m. However, a gravel bed appears again at a depth of about 15 m. This strongly indicates that the seabed in this area was covered with coarse sand and gravel in the past, but the zone at a depth near the depth of closure had been covered with fine sand as the shoreline advanced in recent years. Namely, it is assumed that there are two "conveyer belts", each carrying mainly gravel and fine sand alongshore in zones shallower and deeper than approximately 3 m, respectively, and that the conveyer belt carrying gravel moved offshore because of the accretion of gravel near the shoreline, causing the offshore movement of the longitudinal profile, as schematically shown in Fig. 23; simultaneously, the other conveyer belt carrying fine sand was pushed offshore, resulting in the offshore gravel bed being covered with fine sand.

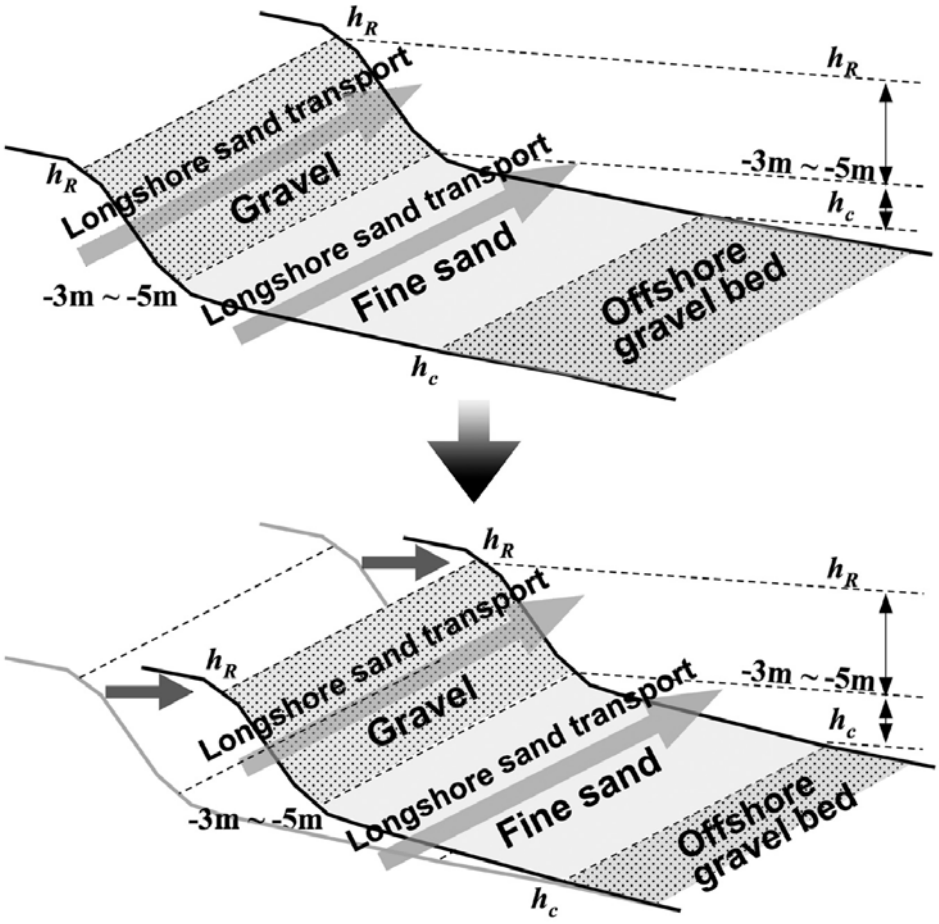

Fig. 23. Schematical explanation of conveyer belts, each carrying mainly gravel and fine sand

Along transect No. 27 located north of the L-groin, where the shoreline significantly retreated after the construction of the groin (Fig. 22(f)), the beach slope between the shoreline and a depth of 30 m is as steep as 1/6. Major beach changes are observed up to a

depth of 10 m. The depth zone in which beach erosion occurred is covered with gravel, the median diameter of which ranges between 20 and 30 mm, but the seabed surface in the zone deeper than 10 m is covered with fine sand with d_{50}=0.2 mm, which are the same features as those along transect No. 32, despite the steep slope in the offshore zone.

5.3 Calculation conditions

In the numerical prediction of beach changes, the difference in the equilibrium slope between the zones composed of gravel and fine sand must be taken into account. Before the construction of the artificial headlands, longshore sand was continuously transported alongshore at a constant rate, because no beach changes were observed in this area, i.e., the coast was under a dynamically stable condition; thus, a dynamically stable beach (Uda et al., 2007) was reproduced. In Fig. 24, the shoreline orientation gradually rotates counterclockwise and shifts by 20º between the south and north ends of the study area. The predominant wave direction of this coast is south, and under this oblique wave incidence, Snell's law gives a breaker angle of α_b=17º at the south end of the calculation domain (Uda et al., 2007). Taking this shift of the shoreline orientation into account, we change the incident angle of the waves linearly from south to north in the calculation domain. In this case, the wave height was decreased alongshore corresponding to the change in the wave direction, so that longshore sand transport flux remained constant before the construction of the headlands and that a dynamically stable beach could be simulated.

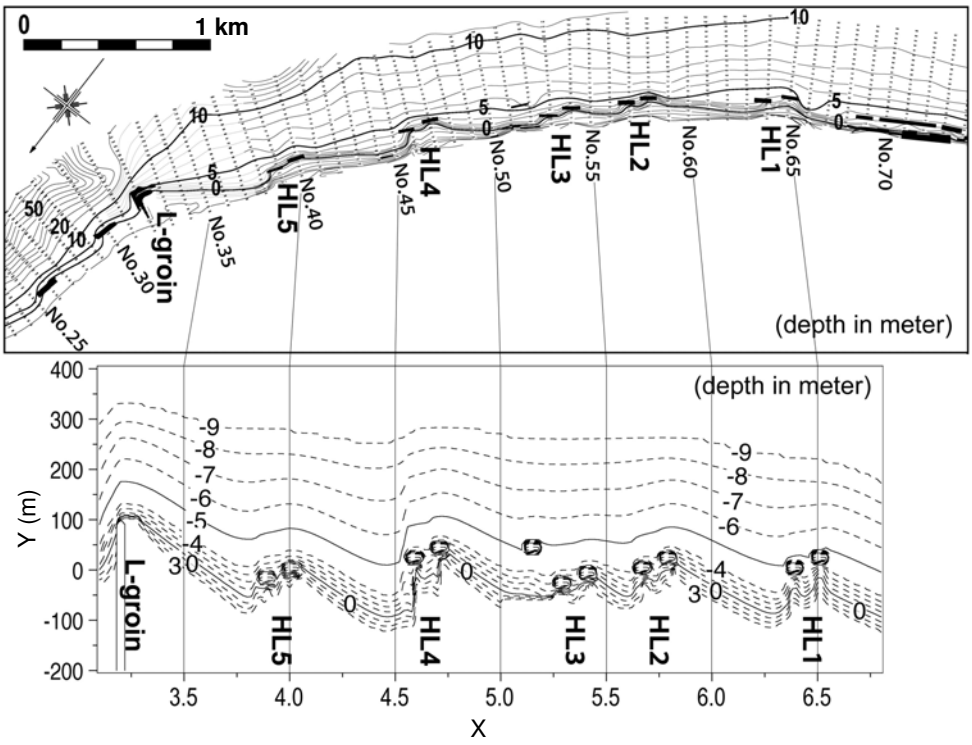

Fig. 24. Calculation domain

As the wave conditions, rough waves with a 5% probability of occurrence are selected on the basis of the results of wave observation off the Shimizu coast; beach changes are more significantly affected by rough waves than normal waves. The selected equivalent wave height H_0' and the wave period are 3 m and 9 s, respectively. The detached breakwaters were placed on this dynamically stable beach, and rough waves were generated for 15 years. Because the seabed is separated into a steep slope mainly composed of gravel in the zone shallower than 4 m and a gentle slope mainly composed of fine sand in the zone deeper than 4 m, as shown in Fig. 22, the changes in the grain size of the sand were implicitly modeled by the changes in the equilibrium slope, which depends on the grain size, by applying the contour-line-change model (Serizawa et al., 2003). In this study, the effect of the difference in grain size was implicitly included as the difference in the equilibrium slope in the ordinary contour-line-change model, assuming that the beach changes take place without the rapid mixing of sand between the beach near the shoreline and the offshore seabed, which are mainly composed of gravel and fine sand, respectively. Table 2 shows the calculation conditions.

Given the topography in 1983 before beach erosion as the initial condition, beach changes until 2006 were predicted while increasing the number of artificial headlands with time. The initial topography with straight parallel contours is set using an expanded coordinate system, to which curvilinear coordinates fixed along the shoreline in 1989 are assigned, in accordance with the method of Uda et al. (1998). The x-axis is taken to be alongshore and the y-axis is perpendicular to the x-axis. The beach slope was assumed to be 1/10 in the depth zone between +3 and -4 m, and 1/50 in the zone deeper than -4 m on the basis of the measured profiles. The depth of 4 m is a critical depth dividing the depth zones. The berm height h_R and depth of closure h_c were assumed to be 3 and -7 m, respectively, for the coarse sand forming a steep slope off the shoreline. To take into account the gradual beach changes observed in the zone deeper than 8 m, the movement of fine sand, mainly covering the seabed depth zone between 8 and 9 m, as typically shown in Fig. 22(d), must be considered. In this study, the depth distribution given by Uda and Kawano (1996) was used for the depth distribution of longshore sand transport in the depth zone between the berm height and 7 m depth, and a constant distribution of longshore sand transport accounting for 3% of all the total sand transport was assumed in the depth zone between 8 and 9 m. For the calculation in the vertical direction, the depth range between z=-7.5 m and z=3.5 m was divided into cells with Δz=1 m. Since the seabed slope in the offshore zone is as gentle as 1/50, there is no sinking of sand to a deeper zone.

As a boundary condition, the longshore sand transport Q_{in} of 1.3×10^5 m^3/yr is introduced at the right boundary of the calculation domain between 1983 and 1990 as a natural condition; after 1990, 3.5×10^4 m^3/yr is assumed as the rate of natural sand supply from upcoast and from beach nourishment. At the left boundary, a free boundary permitting the transport of longshore sand is set; longshore sand transport along each contour line is invariant. Beach nourishment provides the source of sand at the shoreline. The coefficient of longshore sand transport is adjusted so that Q at any point along the initial shoreline is equal to Q_{in}, satisfying the condition that the same amount of longshore sand transport as the inflow flows out through the left boundary. For this purpose, the coefficient of longshore sand transport K_x is selected to be 0.0059, which is two orders of magnitude smaller than the typical value. This is because the continuous action of rough waves that occur with a low probability throughout the year is assumed. The distances between the shoreline and the artificial headlands are given by the distances measured relative to the shoreline position in 1983. The wave sheltering effect of the artificial headlands is evaluated by the angular spreading method for irregular waves given by Sakai et al. (2006).

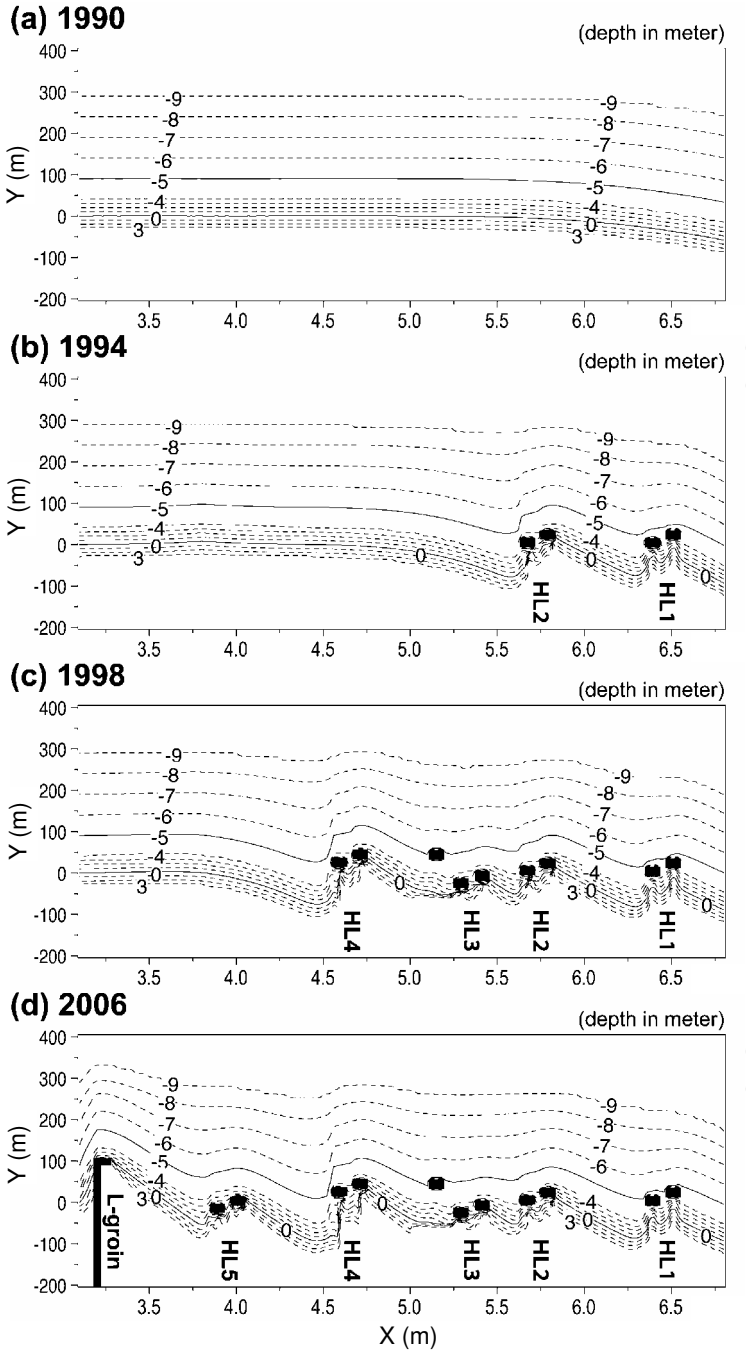

Fig. 25. Predicted bathymetries ((a) 1990, (b) 1994, (c) 1998, and (d) 2006)

Initial topography	Straight parallel contours (shoreline in 1983)
	Uniform slopes of tanβ=1/10 in depth zone shallower than -4 m and tanβ=1/50 in depth zone deeper than -4 m
Wave conditions	Breaker height: H_0'=3 m and T=9 s
	Breaker angle:α_b=17°(wave direction: south) at south end with linear increase in breaker angle from 17° to 37°
Tide level	Mean sea level
Depth of closure	h_c= -7 and -9 m for coarse and fine sand, respectively
Berm height	h_R=3 m
Coefficients of sand transport	K_x=0.0059 and K_z=0.1K_x
	K_2=1.62K_x (Ozasa and Brampton, 1980)
Depth distribution of sand transport rate	Cubic equation given by Uda and Kawano (1996) between +3 and -7 m, and uniform distribution between -8 and -9 m
Equilibrium slope	tanβ_c=1/10 in depth zone shallower than -4 m
	tanβ_c=1/50 in depth zone deeper than -4 m
Critical slope	1/2 on land and 1/2 on seabed
Calculation domain	z=+3.5 to -9.5 m
Mesh size	Δx=20 m and Δz=1 m
Time interval	Δt=10 h
Total time of calculation	t=10 yr
Boundary conditions	Right boundary: Q_{in}=1.3×10^5 m^3/yr between 1983 and 1990 (natural condition)
	Q_{in}=3.5×10^4 m^3/yr after 1990 (natural sand supply +nourishment)
	Left boundary: free (dq_x/dx =0)
	Landward and offshore boundaries: q_z=0
Wave transmission coefficient	K_t=0.5 for artificial headland
Calculation method	Explicit finite difference method
Calculation of wave field	Angular spreading method (Sakai et al., 2006), S_{max}=25

Table 3. Calculation conditions

5.4 Results

Figure 25(a) shows the predicted bathymetry for 1990 immediately before the construction of HL Nos. 1 and 2. The sea bottom contours started to retreat from the upcoast boundary. Figure 25(b) shows the predicted bathymetry for 1994 after constructing HL Nos. 1 and 2. Since northward longshore sand transport was blocked by the construction of HL Nos. 1 and 2, the contours immediately downcoast of HL retreated, and simultaneously, the offshore contours meandered because of the changing direction of the movement of sand off the detached breakwaters. Figure 25(c) shows the predicted bathymetry for 1998 immediately before the construction of the L-groin. After the construction of the HLs, the eroded zone downcoast of the HLs also propagated northward. Finally, the predicted

bathymetry for 2006 is shown in Fig. 25(d). As a result of the construction of the L-groin, the shoreline advanced south of the L-groin. Upon examining the configuration of the seabed contours around the L-groin in detail in the predicted bathymetry for 2006, as shown in Fig. 25(d), it was found that the shoreline south of the groin advanced up to 100 m after the construction of the groin. This shoreline advance caused the offshore movement of the longitudinal profile in the zone shallower than 7 m, resulting in the further advance of the gentle slope covered with fine sand between the depths of 7 and 9 m. The predicted contours are in good agreement with the measured results shown in Fig. 20. Figure 26 shows the measured and predicted shoreline changes in 1983 and 2006. The predicted shoreline is in good agreement with the measured shoreline, although there are some variations at each headland.

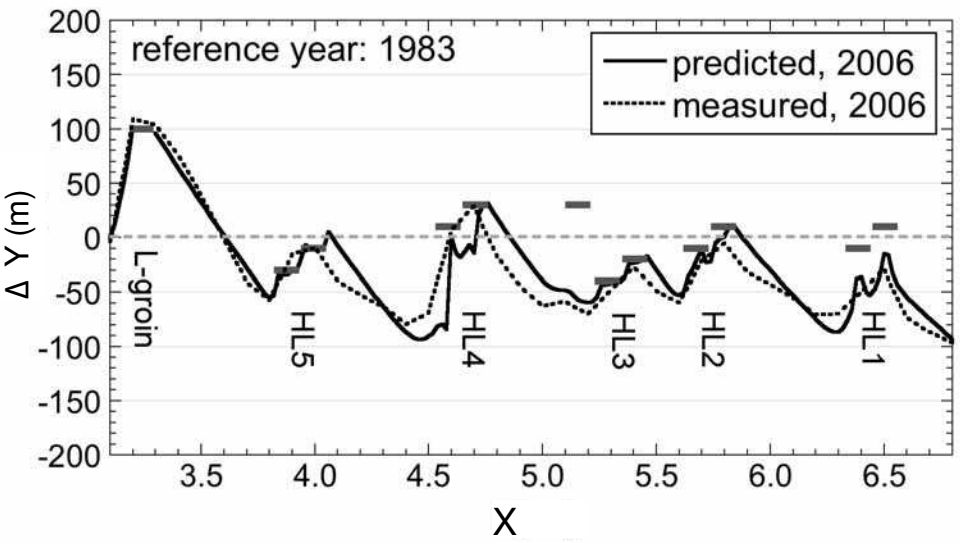

Fig. 26. Measured and predicted shoreline changes

6. Conclusions

A model for predicting the change in the longitudinal profile as well as the change in the grain size distribution was developed using the concept of an equilibrium slope corresponding to each grain size population. The model was applied to the analysis of the results of a large-scale movable bed experiment, and it accurately reproduced the characteristics indicating that sand of mixed grain size is sorted; coarse sand is transported shoreward to form a berm and fine sand is transported offshore to a zone deeper than h_c. It was confirmed that when the content of coarse sand increases, the foreshore becomes wide owing to the formation of a berm, and this contributes to the shoreline advance. In contrast, with an increase in the content of fine sand, the outflow of sand toward a zone deeper than h_c increases. The model was further applied to the Chigasaki coast where beach nourishment using materials of mixed grain sizes was carried out. It was concluded that the optimum method of nourishment was to use sand of mixed grain sizes containing coarse

and fine sand particles, although nourishment using gravel was effective for protecting the shoreline zone. In the third example, the model was applied to the Shimizu coast, where conveyer belts mainly carrying gravel and fine sand were found. The three-dimensional beach changes between 1983 and 2006 were predicted by this model, and the predicted shoreline changes were in good agreement with the measured values. Finally, it is concluded that the present model is highly applicable to predicting beach changes and grain size changes.

7. References

Bakker, W. T. 1968. The dynamics of a coast with a groyne system, *Proc. 11th ICCE*, pp. 492-517.

Fukuhama, M., T. Uda, M. Serizawa and T. Ishikawa. 2007. Change in longitudinal profile using sand of mixed grain size in large wave tank and its numerical simulation, *Coastal Sediments '07*, pp. 259-271.

Kamphuis, J. W., M. H. Davies, R. B. Narim and O. J. Sayao. 1986. Calculation of littoral sand transport rate, *Coastal Engineering*, Vol. 10, pp. 1-12.

Kraus, N. C. 1985. Field experiments on vertical mixing of sand in the surf zone, *J. Sedimentary Petrology*, Vol. 55, pp. 3-14.

Kumada, T., A. Kobayashi, T. Uda and M. Serizawa. 2003. Development of predictive model of shoreline and grain size changes, *Coastal Sediments '03*, pp. 1-14.

Meguro, S., K. Yamamoto and K. Fukuhama. 2005. Formation process of equilibrium beach responding to grain size of beach nourishment, *Annual J. Coastal Eng. JSCE*, Vol. 52, pp. 501-505. (in Japanese)

Nishitani, M., T. Uda, M. Serizawa and T. Ishikawa. 2008. Measurement and prediction of deformation of conveyer belts carrying gravel and fine sand off Shimizu coast, *Proc. 31st ICCE*, pp. 2570-2582.

Ozasa, H. and A. H. Brampton. 1980. Model for predicting the shoreline evolution of beaches backed by seawalls, *Coastal Eng.*, Vol. 4, pp. 47-64.

Sakai, K., T. Uda, M. Serizawa, T. Kumada and Y. Kanda. 2006. Model for predicting three-dimensional sea bottom topography of statically stable beach, *Proc. 30th ICCE*, pp. 3184-3196.

Serizawa, M., T. Uda, T. San-nami, K. Furuike and T. Kumada. 2003. Improvement of contour line change model in terms of stabilization mechanism of longitudinal profile, *Coastal Sediments '03*, pp. 1-15.

Uda, T. and S. Kawano. 1996. Development of a predictive model of contour line change due to wave, *Proc. JSCE*, No. 539/II-35, pp. 121-139. (in Japanese)

Uda, T., M. Sumiya, H. Yazawa, Y. Ohtani and Y. Atsusaka. 1998. Prediction of beach changes around Oyazawa-bana sand spit using expanded coordinate system, *Annual J. Coastal Eng.*, JSCE, Vol. 45, pp. 541-545. (in Japanese)

Uda, T., T. Kumada and M. Serizawa. 2004. Predictive model of change in longitudinal profile in beach nourishment using sand of mixed grain size, *Proc. 29th ICCE*, pp. 3378-3390.

Uda, T., M. Serizawa and T. Ishikawa. 2007. Evaluation of controlling effect of sand transport by detached breakwaters built on dynamically stable beach, *Coastal Sediments '07*, pp. 2460-2472.

Yoshioka, A., T. Uda, G. Aoshima, K. Furuike and T. Ishikawa. 2008. Field experiment of beach nourishment considering changes in grain size and prediction of beach changes, *Proc. 31st ICCE*, pp. 2694-2706.

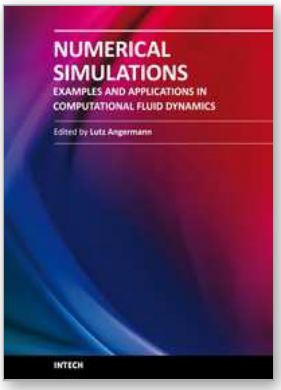

Numerical Simulations - Examples and Applications in Computational Fluid Dynamics

Edited by Prof. Lutz Angermann

ISBN 978-953-307-153-4
Hard cover, 440 pages
Publisher InTech
Published online 30, November, 2010
Published in print edition November, 2010

This book will interest researchers, scientists, engineers and graduate students in many disciplines, who make use of mathematical modeling and computer simulation. Although it represents only a small sample of the research activity on numerical simulations, the book will certainly serve as a valuable tool for researchers interested in getting involved in this multidisciplinary ï¬eld. It will be useful to encourage further experimental and theoretical researches in the above mentioned areas of numerical simulation.

How to reference

In order to correctly reference this scholarly work, feel free to copy and paste the following:

Takaaki Uda and Masumi Serizawa (2010). Model for Predicting Topographic Changes on Coast Composed of Sand of Mixed Grain Size and Its Applications, Numerical Simulations - Examples and Applications in Computational Fluid Dynamics, Prof. Lutz Angermann (Ed.), ISBN: 978-953-307-153-4, InTech, Available from: http://www.intechopen.com/books/numerical-simulations-examples-and-applications-in-computational-fluid-dynamics/model-for-predicting-topographic-changes-on-coast-composed-of-sand-of-mixed-grain-size-and-its-appli

INTECH
open science | open minds

InTech Europe
University Campus STeP Ri
Slavka Krautzeka 83/A
51000 Rijeka, Croatia
Phone: +385 (51) 770 447
Fax: +385 (51) 686 166
www.intechopen.com

InTech China
Unit 405, Office Block, Hotel Equatorial Shanghai
No.65, Yan An Road (West), Shanghai, 200040, China
中国上海市延安西路65号上海国际贵都大饭店办公楼405单元
Phone: +86-21-62489820
Fax: +86-21-62489821